Factors causing climatologically high temperatures in a hottest city in Japan: a multi-scale analysis of Tajimi

doi: 10.1002/joc.4790

INTERNATIONAL JOURNAL OF CLIMATOLOGY
Int. J. Climatol. **37**: 1456–1473 (2017)
Published online 15 June 2016 in Wiley Online Library
(wileyonlinelibrary.com) DOI: 10.1002/joc.4790

RMetS
Royal Meteorological Society

Factors causing climatologically high temperatures in a hottest city in Japan: a multi-scale analysis of Tajimi

Yuya Takane,[a]* Hiroyuki Kusaka,[b] Hiroaki Kondo,[a] Maki Okada,[c,†] Midori Takaki,[c,‡] Shiori Abe,[c,§] Shota Tanaka,[c,¶] Kenji Miyamoto,[d] Yukino Fuji[d] and Toru Nagai[d]

[a] *Environmental Management Research Institute, National Institute of Advanced Industrial Science and Technology, Tsukuba, Japan*
[b] *Center for Computational Sciences, University of Tsukuba, Japan*
[c] *Graduate School of Life and Environmental Sciences, University of Tsukuba, Japan*
[d] *Environmental Division, Tajimi City Government, Japan*

ABSTRACT: In this study, multi-scale climatological features of extreme high temperature (EHT) events in Tajimi, the hottest cities in Japan, were investigated using observational data collected by the Japan Meteorological Agency over the past 23 years, and original data observed by the authors over the last 3 years. Results revealed the background factors that lead to climatologically high temperatures in Tajimi: the occurrence of a characteristic pressure pattern called 'whale': the synoptic-scale factors, and the urbanization of Tajimi: the meso-γ-scale factors. In addition, the high temperatures measured in Tajimi are affected by the foehn-like westerly airflow coming from the mountains located in the northwest/west towards the Nobi Plain where Tajimi is located at the east end: the meso-β-scale factors, and the location of the Tajimi observation site, which is within an urbanized area where the highest temperatures tend to be observed: the micro-scale factors. In contrast, statistical analysis demonstrated that the small-scale basin effects and soil dryness around Tajimi were of lesser importance than aforementioned factors, in the occurrence of EHT events in Tajimi.

KEY WORDS extreme high temperature; pressure pattern; foehn wind; statistical analysis; urban climate

Received 25 May 2015; Revised 28 April 2016; Accepted 6 May 2016

1. Introduction

Extreme high temperature (EHT) events relating to climate change have become a social problem, because such events have a significant impact on human health, agriculture, and energy demands. Numerous impact assessment studies have been conducted to investigate the effects of such events on human activity (De Bono *et al.*, 2004; Ciais *et al.*, 2005; IPCC, 2014).

EHT events are generally known to be triggered by multi-scale factors at global, synoptic, meso-, and micro-scales. From a global-scale perspective, Schär *et al.* (2004) and Beniston (2004) showed that the European warm anomaly during the summer of 2003 was statistically unusual at three times the standard deviation, and that the anomaly was related to a deep tropospheric phenomenon (Chase *et al.*, 2006). Looking from the synoptic-scale standpoint, Black *et al.* (2004) and Fink *et al.* (2004) stated that anticyclonic synoptic weather during the summer of 2003 caused dry conditions, which continuously reduced soil moisture content. This dry surface condition contributed to the high temperatures in Europe during the summer of 2003, enhancing the surface sensible heat flux. Takane *et al.* (2013) showed that the inflow of sensible heat transported by synoptic-scale winds from the Tropics under a typical summer pressure pattern in Japan is one of the factors causing meso-scale high temperatures in the Osaka and Kyoto urban areas. Urban heat islands (UHI) in the metropolitan areas (Grossman-Clarke *et al.*, 2010; Li and Bou-Zeid, 2013), and foehn winds associated with airflow over the mountains (Takane and Kusaka, 2011; Takane *et al.*, 2015), have been classified as meso-scale factors. Deteriorated ventilation due to the construction of buildings, tree growth, and other effects on the localized temperature increase around observation sites [the 'Hidamari (suntrap) effect'] have been suggested by Kondo (http://www.asahi-net.or.jp/~RK7J-KNDU/) (in Japanese) as micro-scale factors.

Record-breaking EHT events have occurred in various areas of Japan, and the factors contributing to these events have been investigated from mainly synoptic and meso-scale viewpoints. For instance, Yamagata City, located in the Tohoku region (Figure 1(a)), recorded a high temperature of 40.8 °C on 25 July 1933, breaking the highest daily maximum temperature previously recorded. It has been demonstrated that the meso-scale foehn

* Correspondence to: Y. Takane, Environmental Management Research Institute, National Institute of Advanced Industrial Science and Technology, 16-1 Onogawa, Tsukuba, Ibaraki 305-8569, Japan. E-mail: takane.yuya@aist.go.jp

†Current affiliation: Japan Weather Association, Tokyo, Japan.
‡Current affiliation: City of Yokohama, Japan.
§Current affiliation: Mitsui Consultants Co., Ltd., Tokyo, Japan.
¶Current affiliation: NHK Enterprises, Inc., Tokyo, Japan.

wind from the central ridge in northeast Japan played a primary role in this high temperature event [Japan Meteorological Agency (JMA), http://www.jma-net.go.jp/sendai/wadai/kikouhenka/column&uscore;yamagata.html (in Japanese)]. On 12 August 2013, Shimanto City in Kochi Prefecture (Shikoku island) (Figure 1(a)) recorded a temperature of 41.0 °C, the highest daily maximum temperature ever recorded in Japan. This event was linked to a distinctive synoptic-scale pressure pattern, together with the meso-scale flow. On 16 August 2007, Kumagaya City in Saitama Prefecture, located in the Kanto Plain, which includes the Tokyo metropolitan area (Figure 1(a)), recorded a temperature of 40.9 °C (breaking the previously recorded highest daily maximum temperature). The mechanism underlying this high temperature event was investigated by Takane and Kusaka (2011), who revealed that the record-breaking temperature was caused by a type of foehn-like wind that induced high surface temperatures on the leeward side. Takane *et al.* (2014) have also investigated the climatological features of EHT events in the inland area of the Kanto Plain. Their study shows that three characteristics are apparent when high temperatures are observed in the inland area of the Kanto Plain: (1) the occurrence of a 'whale' (tail of a whale) synoptic-scale pressure pattern, (2) consecutive clear-sky days prior to EHT events, and (3) prominent daytime northwesterly meso-scale surface (foehn) winds. These findings show that consecutive clear-sky days and northwesterly meso-scale (foehn) winds under this distinctive synoptic-scale pressure pattern play a role in the occurrence of EHT events in the inland area of the Kanto Plain.

A high temperature of 40.9 °C was recorded on 16 August 2007 in Tajimi City, Gifu Prefecture (Figure 1), which is located on the periphery of the Nagoya metropolitan area (the north-eastern area of the Nobi Plain). Tajimi is located in a small-scale basin, 10 km in diameter, and is surrounded by mountains lower than 400-m elevation (Figure 2(a) and (c)). The city is spread out in the basin (Figure 2(b) and (d)), and is relatively small. There are high buildings in downtown Tajimi (no. 10 in Figure 2(c); Figure 2(e)). However, the suburbs of the city are characterized by relatively low buildings (Figure 2(e)). The green fraction is very low at the bottom of the Tajimi basin (Figure 2(f)). The Toki River flows from northeast of the city towards the south (where downtown Tajimi is located) (Figure 2(g)). With such geographical conditions, EHT events occur more frequently in Tajimi City than in any other city in Japan, including the aforementioned Kumagaya City (Table 1).

At least seven hypotheses for the cause of the EHT events in Tajimi have been proposed in previous surveys and studies, ranging from synoptic to micro-scale explanations. The EHT events in Tajimi differ from the aforementioned events in Yamagata, Shimanto, and Kumagaya, in that the Tajimi events have involved multi-scale factors including those on the micro-scale in addition to the synoptic and meso-scale. The hypotheses

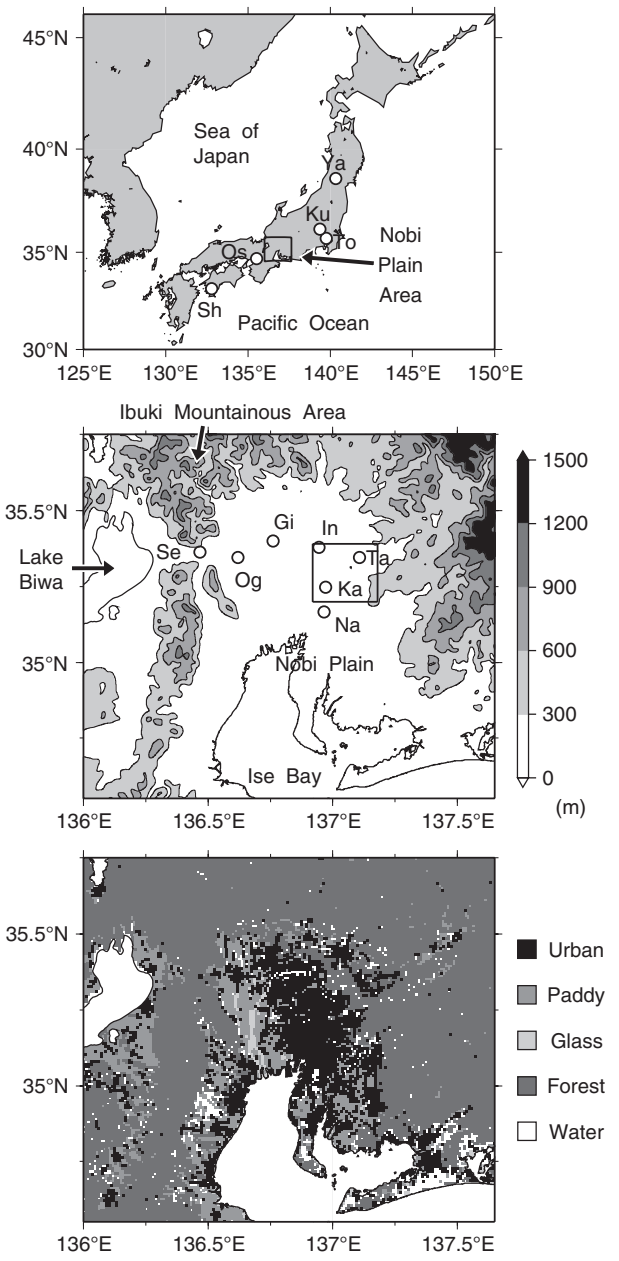

Figure 1. Map of Japan with inset of Nobi Plain area (a) with site locations: Yamagata (Ya), Kumagaya (Ku), Tokyo (To), Osaka (Os), and Shimanto (Sh). (b) and (c) show topography and land-use categories (respectively) in the Nobi Plain area with site locations of the analysed sites: Tajimi (Ta), Nagoya (Na), Gifu (Gi), Ogaki (Og), Inuyama (In), Kasugai (Ka), and Sekigahara (Se).

associated with the EHT events in Tajimi include the following. (1) A characteristic pressure pattern (Figure 3(a)). Onuma (2003) illustrated the presence of a characteristic pressure pattern that triggers high temperatures in the Nobi Plain, and analysed several EHT events. (2) Airflow coming from the mountains located on the western/northwestern side (Figures 3(b) and 4). Onuma (2003) indicated the high possibility of a traditional foehn wind (Hann, 1866; Seibert, 1990) when EHT events occur in the Nobi Plain. Additional studies are necessary to elucidate the climatological features in the hypotheses (1) and (2), because research to date has been based only on

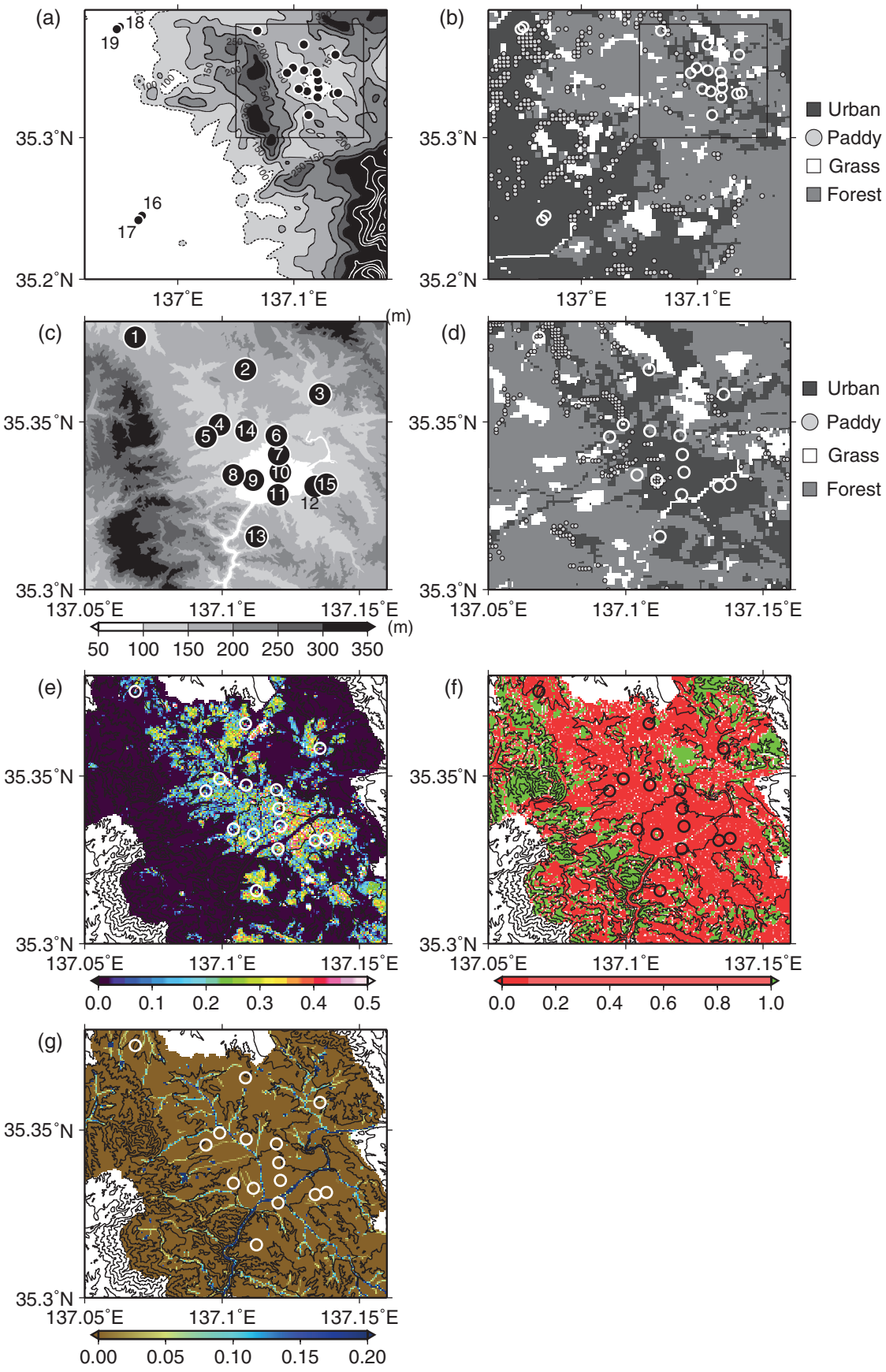

Figure 2. (a) and (c) Topography, (b) and (d) land-use categories, (e) building coverage, (f) green fraction, and (g) water fraction in and around Tajimi City, with locations [circles with numbers in (c) and open circles in (d)–(g)] of observational sites 1–19 in Table 2.

Table 1. Frequency of EHT evets (over 38.1 °C) at Tajimi, Nagoya, Gifu, Kumagaya, and Tokyo sites from July to August 1990–2012.

	Tajimi	Nagoya	Gifu	Kumagaya	Tokyo
Frequency	49	15	27	29	5

case study analysis. (3) Heat transport from the Nagoya metropolitan area (Figures 3(b) and 4). Numerical simulations conducted by Ito *et al.* (2012) using the weather research and forecasting model (Skamarock *et al.*, 2008) showed that heat transport from the Nagoya metropolitan area had no effect on Tajimi City between August 2006 and 2010. However, the possibility of heat transport from Nagoya City was not examined from observational and climatological perspectives. (4) Basin effects. In addition to small-scale foehns associated with airflow over the basin terrain (Figure 3(c)), thermally induced local circulation (valley winds) raised the temperature in the basin under weak synoptic-scale wind conditions (Kondo *et al.*, 1989; Kuwagata and Kimura, 1997), and trapped heat within the basin during daytime. (5) The UHI effect in Tajimi [Figure 3(c); e.g. as described by Okada *et al.* (2014)]. Numerical simulations conducted by Ito *et al.* (2012) indicate that the UHI effect is a factor in EHT events in Tajimi. However, it is still unclear whether the UHI effect in Tajimi causes the highest temperatures in the Nobi Plain, considering that other adjacent cities have larger urban area than Tajimi City. (6) Soil dryness (Fujibe, 1996; Black *et al.*, 2004; Fink *et al.*, 2004; Yoshida, 2013), and (7) the local thermal environment around Tajimi, as recorded by the Automated Meteorological Data Acquisition System (AMeDAS) site operated by the JMA (Figure 3(d), e.g. Kondo, http://www.asahi-net.or.jp/~RK7J-KNDU/). Hypotheses (4), (6), and (7) have been reported by citizens' groups (e.g. Kondo, http://www.asahi-net.or.jp/~RK7J-KNDU/, in Japanese) to explain the occurrence of EHT events. However, the actual conditions involved in these three hypotheses are

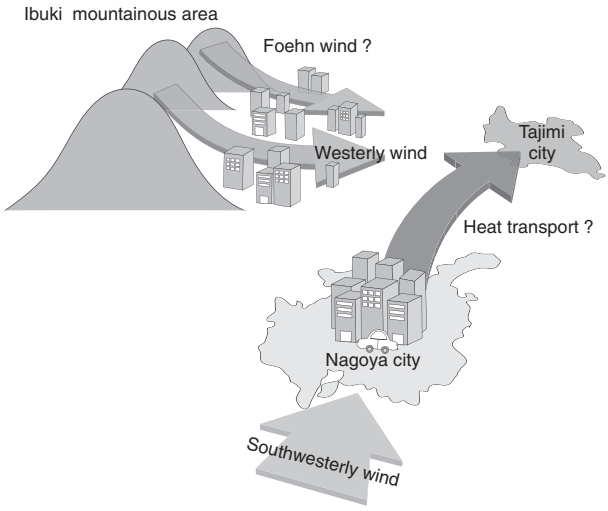

Figure 4. Schematic representation of the meso-β-scale winds, westerly and southwesterly on the Nobi Plain.

unknown, because no detailed investigation has been conducted. Accordingly, the seven hypotheses regarding factors on various scales, considered to be related to EHT events in Tajimi, have not yet been examined through statistical analyses. Therefore, the climatological features and actual conditions of the EHT events have yet to be elucidated.

In this study, we examine the seven hypotheses proposed to explain the EHT events in Tajimi from an observational perspective. The results should help to elucidate the multi-scale climatological conditions for EHT events on the Nobi Plain, and may be applicable to EHT events occurring in other regions and other small cities in complex terrain.

2. Data and concept of this study

The data used in this study include the following: surface weather charts [fax chart(s) SPAS and ASAS by JMA]

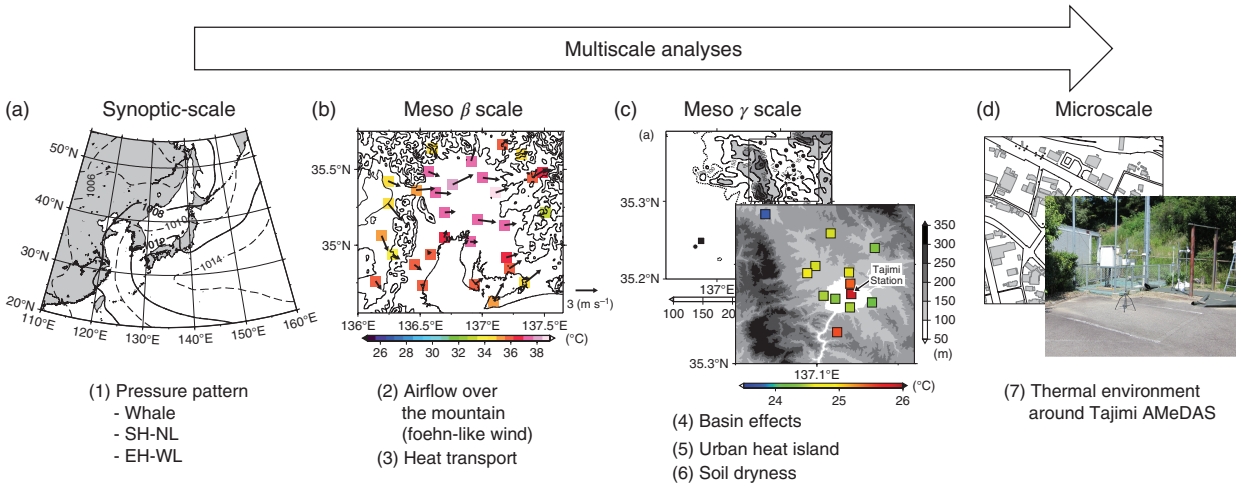

Figure 3. Concept of multi-scale analyses used in this study. Numbers refer to the seven hypotheses outlined in Section 1.

Table 2. Information relating to observation sites.

Site number	Site name	City	Height above ground level (m)	Surface	Local environment	Observation year
1	Minamihime JHS	Tajimi	160	Bare land	School yard	2010 and 2011
2	Hokuei JS	Tajimi	193	Grass land	School yard and building	2010 and 2011
3	Kyouei JS	Tajimi	159	Grass land	School yard and building	2010 and 2011
4	Koizumi Park	Tajimi	117	Grass land	Park surrounded by trees	2010, 2011, and 2012
5	Koizumi JHS	Tajimi	131	Concrete	School yard and building	2010 and 2011
6	Touto JHS	Tajimi	106	Bare land	School yard	2010 and 2011
7	Seika JS	Tajimi	98	Bare land	School yard	2010 and 2011
8	Ikeda JS	Tajimi	126	Bare land	School yard	2010 and 2011
9	Taihei Park	Tajimi	94	Grass land	Park surrounded by trees	2010, 2011, and 2012
10	Tajimi JR Station	Tajimi	95	Asphalt	Built-up area	2010 and 2011
11	Shouwa JS	Tajimi	95	Bare land	School yard	2010 and 2011
12	Yousei JS	Tajimi	123	Concrete	School yard and building	2010 and 2011
13	Wakinoshima JS	Tajimi	182	Bare land	School yard	2010 and 2011
14	near AMeDAS	Tajimi	105	Asphalt	Parking area	2011
15	Minamisakaue Park	Tajimi	121	Grass land	Park surrounded by trees	2011 and 2012
16	Harumi Park	Kasugai	26	Grass land	Park surrounded by trees	2010
17	Kasugai Central Park	Kasugai	23	Grass land	Park surrounded by trees	2011 and 2012
18	Ishizukuri Park	Inuyama	53	Bare land	Park surrounded by trees	2011 and 2012
19	Nakayama Park	Inuyama	52	Grass land	Park surrounded by trees	2011 and 2012

recorded at 0900 Japan Standard Time (JST: UTC + 9 h); aerological (850, 700, 500, and 300-hPa pressure levels) weather charts [fax chart(s) AUPQ78 and AUPQ35 by JMA] at the same time; AMeDAS data provided by the JMA; objective analysis data with a T106L40 resolution and 6-h temporal resolution: Japanese 25-year Reanalysis (JRA-25) data and the JMA Climate Data Assimilation System (JCDAS) (hereafter referred to as 'JRA-25/JCDAS') (Onogi *et al.*, 2007) provided by the JMA and the Central Research Institute of the Electric Power Industry; and JMA meso-scale model (hereafter MSM) objective analysis data with 5-km resolution and 3-h temporal resolution. Original temperature observation data were also collected by the authors in August 2010, during July–August 2011, and July–August 2012.

Figure 2(a) and (c) shows the sites where observations were made with site numbers: information on each site is described in Table 2. A portable thermistor thermometer and data logger (Ondotori Jr. RTR-52; T&D Company, Ltd.) mounted in a radiation shelter (Sakai *et al.*, 2009) was used to record air temperature at 1.5 m above ground level. The recording interval was set to be 2 min, and the average values recorded over 10 min before and after the observation time (11 samples) were used for analysis. Since the elevation of the observation sites was different, an altitude correction for temperature was implemented; the observed temperatures were corrected a height of 95 m (site number 10 in Figure 2(a) and in Table 2) using a temperature lapse rate of 0.0065 °C m^{-1}. Hereafter, the temperatures obtained in our observations are as the values after altitude correction.

This study uses the terms 'clear-sky days' and 'EHT days' in the analysis, following the definitions in Takane *et al.* (2014). A 'clear-sky day' was defined as a day when the duration of sunshine at the Tajimi AMeDAS site was longer than 6 h without precipitation (553 of 1426 days in the entire analysis period). An 'EHT day' was defined as a day with a daily maximum temperature over 38.1 °C, which is 1.5 times sigma above the mean daily maximum temperature at Tajimi AMeDAS site during the analysis period (Figure 5(a)) (49 of 1426 days). No trend, either increasing or decreasing, was found in the number of clear-sky days during 1990 and 2012 (Figure 5(b)). Although the number of EHT days varied each year, during the 1990s (1990–1999) EHT days were observed only in 1994 and 1995, while EHT days were recorded almost every year after 2000 (2000–2012), except in 2003, 2005, and 2009.

3. Results

3.1. Synoptic-scale

This sub-section describes the investigation of hypothesis (1): that a characteristic pressure pattern is linked to the occurrence of EHT days (Figure 3(a)). As described in the introduction, based on a climatological analysis, Takane *et al.* (2014) discussed the possibility that EHT events in the inland area of the Kanto Plain were related to background temperature rises caused by the 'whale' pressure pattern (Figure 6(a)) that generated northwesterly synoptic-scale and foehn winds. However, Onuma (2003) indicated that the 'whale' pressure pattern was found in only a few EHT cases in Nagoya and Gifu.

In this study, we first used the classification of 'all days'; i.e. the total numbers of days, 'clear-sky days' and 'EHT days' as in Takane *et al.* (2014). In addition, we classified the surface pressure pattern into ten patterns based on those of the Encyclopaedia of Meteorology and Atmospheric Sciences [Meteorological Society of Japan, 1998; Figure 4 in Takane *et al.* (2014)]. Specifically, pressure patterns for all of the days were manually classified

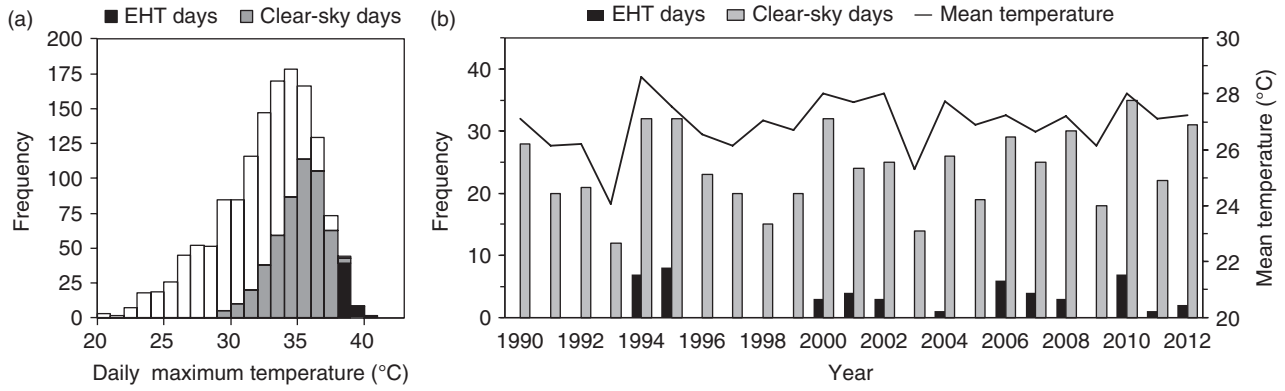

Figure 5. (a) Frequency of daily maximum surface air temperature observed at Tajimi AMeDAS site from July to August 1990–2012. The white bars indicate all days, grey bars clear-sky days, and black bars EHT days. (b) Secular change in clear-sky days, EHT days, and July–August mean temperatures.

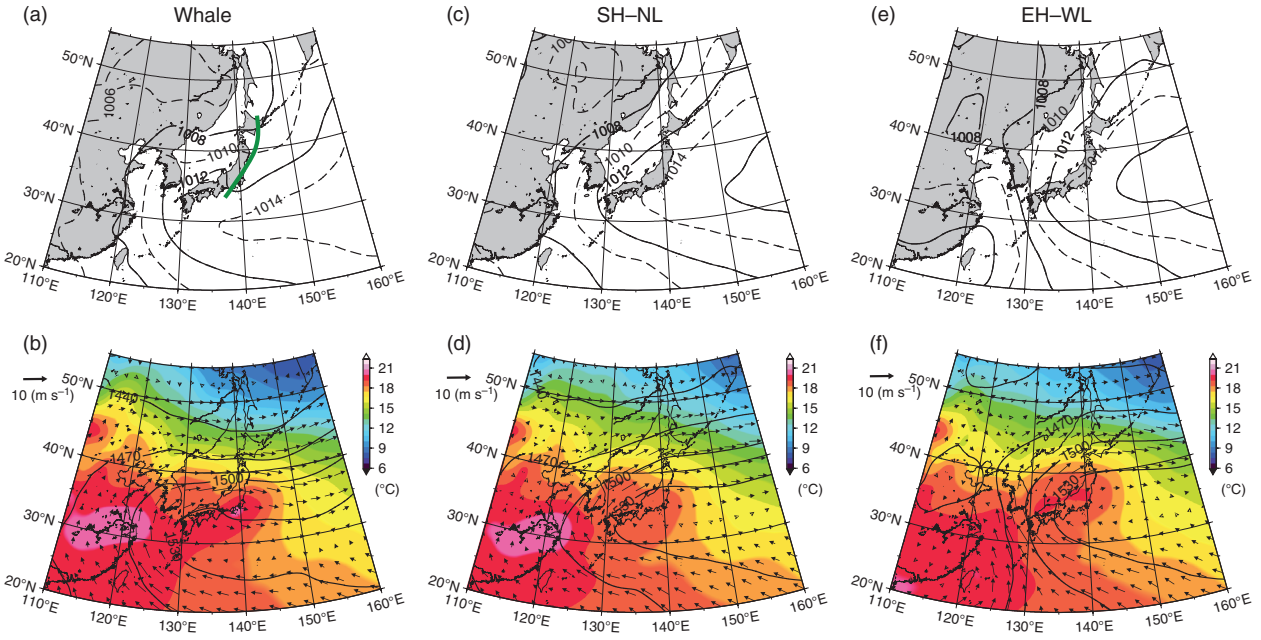

Figure 6. Top: surface pressure (solid line); bottom: geopotential height (solid line), temperature (colour), and horizontal wind (vector) at the 850-hPa pressure level, averaged for clear-sky days using JRA-25/JCDAS. (a) and (b) 'whale', (c) and (d) SH–NL, and (e) and (f) EH–WL. The green solid line in (a) indicates a pressure trough.

based on advice from a professional weather forecaster at the JMA. The results of this classification are shown in Figure 7(a), which describes the high probability of three typical summer pressure patterns in Japan: the 'whale' (tail of a whale), the SH–NL (high pressure in the south and low pressure in the north), and the EH–WL (high pressure in the east and low pressure in the west). All other pressure patterns [NH, MH, ZH, BF, SC, JC, JS-Cs, WH-EL, and Bag in Figure 4 of Takane *et al.* (2014)] are classified as 'other'.

Here, we present the climatological features of surface pressure, geopotential height, wind, and average temperature for 'clear-sky days', for the three selected summer pressure patterns (Figure 6). 'Whale' was associated with a pressure trough in the central part of Japan (Figure 6(a)), which caused a westerly to northwesterly synoptic-scale wind above the area (Figure 6(b)). The average temperature at the 850-hPa pressure level of the 'whale' was higher than that of the SH–NL (Figure 6(b) *vs* (d)). The SH–NL and EH–WL had no pressure trough around central Japan (Figure 6(c) and (e)), and therefore southwesterly synoptic-scale winds blow above central Japan (Figure 6(d) and (f)). In these two pressure patterns, sensible heat is transported from the Tropics along the edge of the Pacific high, as well as from tropical cyclones (in the case of EH–WL) (Takane *et al.*, 2013). Adiabatic compressive heating due to synoptic-scale downward flow, with a high-pressure system, also contributes to high temperatures in central Japan. The average temperatures at 850 hPa with the SH–NL (18–19 °C) and the EH–WL (18–20 °C) were lower than with the 'whale' (19–20 °C). Similar climatological features were obtained for the EHT days for the three summer pressure patterns.

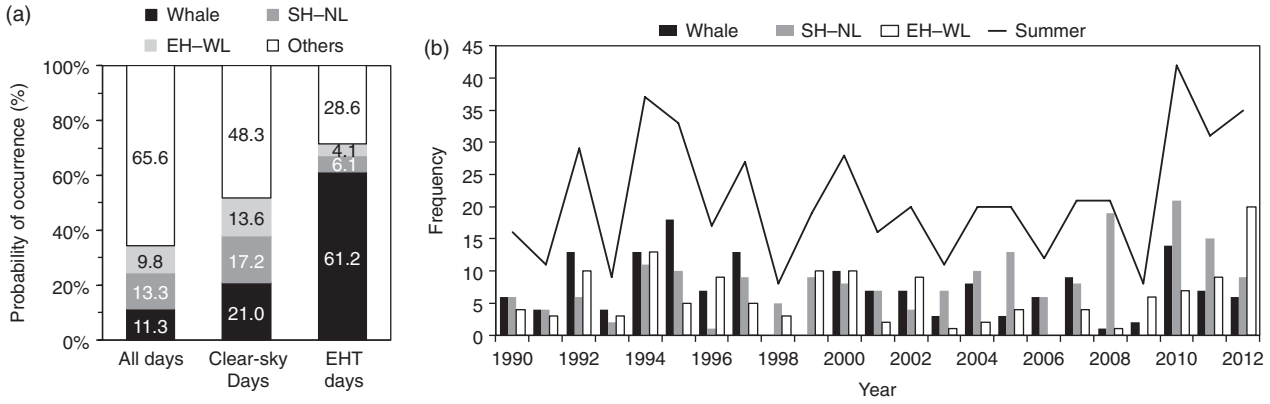

Figure 7. (a) Probability of occurrence of pressure patterns from July to August 1990–2012. (b) Secular change in frequency of 'whale', SH–NL, EH–WL, and summer pressure patterns (sum of 'whale', SH–NL, and EH–WL).

Across all days, the probability of the occurrence of 'whale', SH–NL, EH–WL, and 'other' was 11.3, 13.3, 9.8, and 65.6%, respectively (Figure 7(a)). On clear-sky days, the probability of 'whale' occurring was 21.0% higher than across all days, but was not remarkably higher than the 17.2 and 13.6% for the SH–NL and EH–WL, respectively. On EHT days, the probability of 'whale' occurring was 61.2% (40.2% higher than for clear-sky days). The probability of SH–NL and EH–WL (6.1 and 4.1%, respectively) was lower on EHT days in comparison to clear-sky days. These results indicate that the pressure pattern of 'whale' played a significant role in the high temperatures (EHT days) in Tajimi, but was not sufficient for causing the EHT events. 'Whale' provided the background environment that triggered the higher temperatures in Tajimi.

Figure 7(b) shows the trend in probability of the three summer pressure patterns during 1990–2012: there are no systematic temporal changes in probability for each pattern.

3.2. Meso-β-scale

This section discusses two hypotheses for the cause of the EHT days, hypothesis (2): airflow coming from the mountains located on the western and northwestern sides (Figures 3(b) and 4), and hypothesis (3): heat transport from the Nagoya metropolitan area (Figures 3(b) and 4). Figure 8(a) shows the horizontal distributions of average temperatures and winds at 1400 JST for all days (1426 days), which indicates the prominence of southwesterly winds from the coastal area to the inland area of the Nobi Plain. This characteristic wind was also confirmed as the average wind for clear-sky days (553 days) (Figure 8(b)). However, this southwesterly wind was not apparent for EHT days (49 days) (Figure 8(c)), when a westerly–northwesterly wind blew on the Nobi Plain on which Tajimi is located at the downstream edge. A westerly–northwesterly wind was confirmed on 30 of the 49 EHT days (61.2%).

Figure 9 shows a typical example of an EHT day that occurred on 22 July 2010, when northwesterly winds became prominent on the Nobi Plain. The pressure pattern for the day was 'whale' (Figure 9(a)) and the JMA MSM indicated that northwesterly winds were blowing above the boundary layer in the Nobi Plain at 0900 JST (Figure 9(b)). Under such synoptic-scale conditions, westerly winds were blowing on the ground (Figure 9(c)), passing through Sekigahara from Lake Biwa to the Nobi Plain, and then reaching Tajimi. Northwesterly airflow from the Ibuki mountainous area is also seen in Figure 9(c). This suggests that the westerly–northwesterly winds are deeply related to the EHT events.

Southwesterly winds were prominent on 12 of 49 EHT days (24.5%). Based on these results, it is likely that the airflow coming from the mountains on the northwestern and western sides plays a climatological role in the EHT events [hypothesis (2)]. On the other hand, it is unlikely that heat transport from the Nagoya metropolitan area contributes to the EHT events in Tajimi climatologically [hypothesis (3)], because westerly–northwesterly winds are prominent on EHT days. These results are consistent with the simulation results obtained by Ito *et al.* (2012). However, in this regard, it remains possible that the southwesterly wind, with heat transport from Nagoya, contributed meteorologically to the EHT in Tajimi in several cases, although the southwesterly wind was climatologically not dominant for the EHT events in Tajimi, as mentioned earlier. Further detailed case studies are required to explore this possibility.

3.3. Meso-γ-scale

This section discusses three hypothesis: hypothesis (4): basin effects [small-scale foehns associated with airflow over the mountains surrounding the Tajimi basin, the effects of temperature rise due to thermally induced local circulation (valley wind) under weak synoptic-scale wind conditions, and air stagnation due to blocking of the mountains surrounding Tajimi]; hypothesis (5): UHI in Tajimi; and hypothesis (6): soil dryness (Figure 3(c)).

We first discuss hypothesis (4). As Tajimi is in a small basin surrounded by relatively low mountains (Figure 2(a)), high temperatures might be triggered by small-scale foehns generated by winds crossing over the

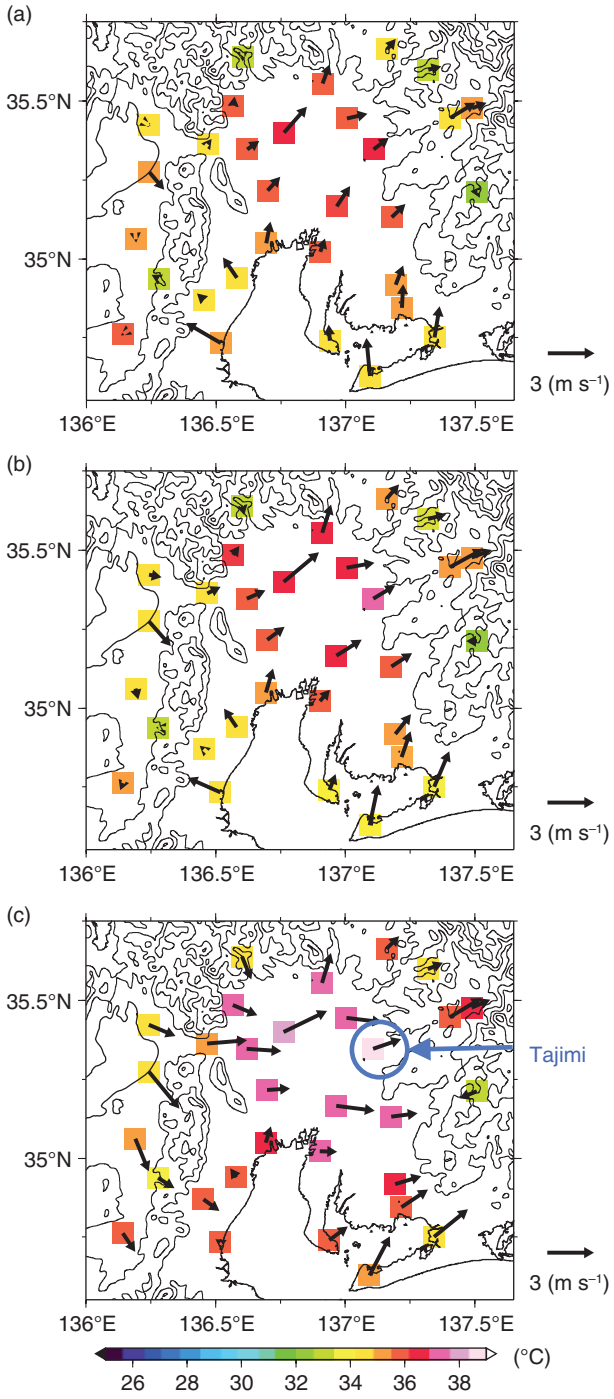

Figure 8. Horizontal distributions of surface air temperature (colour) and wind (vector) at 1400 JST averaged over (a) all days, (b) clear-sky days, and (c) EHT days.

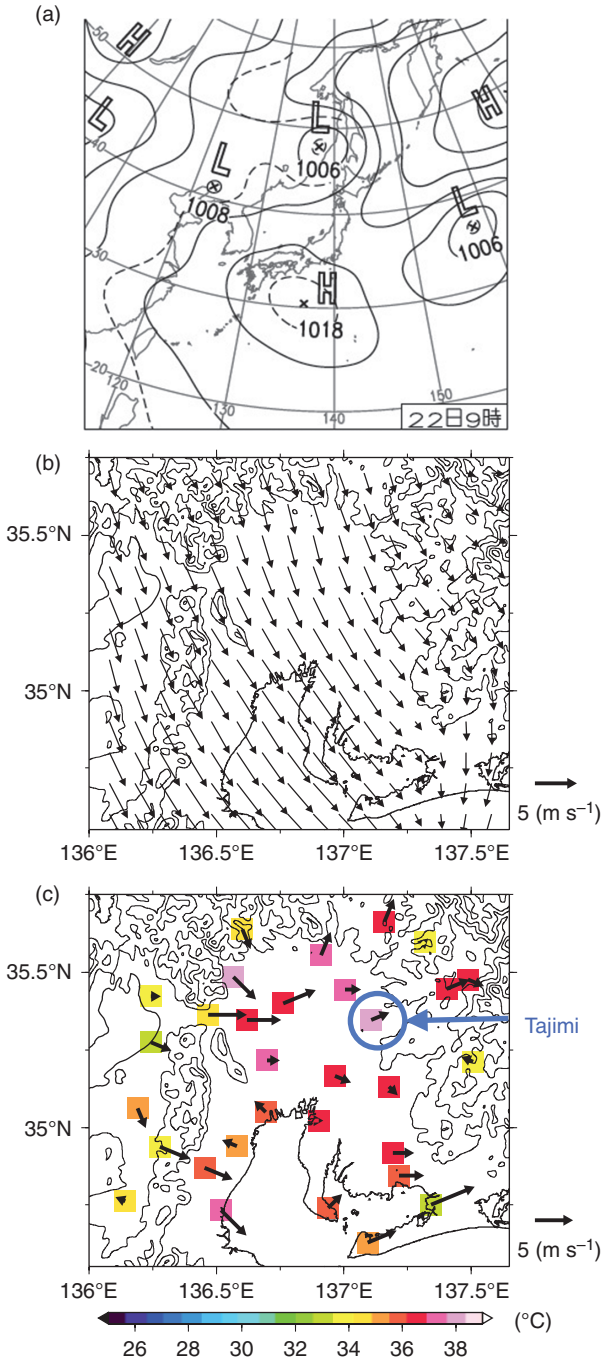

Figure 9. (a) Surface weather chart at 0900 JST on 22 July 2010. (b) Horizontal distribution of wind (vector) at the 850-hPa pressure level at 0900 JST on 22 July 2010 from MSM. (c) Horizontal distributions of surface air temperature (colour) and wind (vector) at 1400 JST on 22 July 2010 from AMeDAS sites.

low mountains when westerly or southwesterly winds blow on the Nobi Plain. To examine this possibility, we conducted fixed point observations of temperature in August 2010 and July–August 2011–2012 at sites in Inuyama (sites 18 and 19) located on the windward side of the prominent westerly wind, in Kasugai (sites 16 and 17), located on the windward side of the southwesterly wind, and in Tajimi (sites 1–15), located on the leeward side.

Figure 10(a) shows 11 cases of prominent southwesterly wind days on the Nobi Plain extracted from the clear-sky days (20 cases) in August 2010. Almost no difference was seen in the daytime temperatures between the two cities, Kasugai and Tajimi. In addition to the cases in August 2010, similar results were obtained for average values in July–August 2011 (Figure 10(b)), and in July–August 2012 (Figure 10(c)).

Figure 10(d) and (e) shows the average temperature obtained in cases of westerly wind on the Nobi Plain (six cases in 2011 and nine in 2012). There was no result

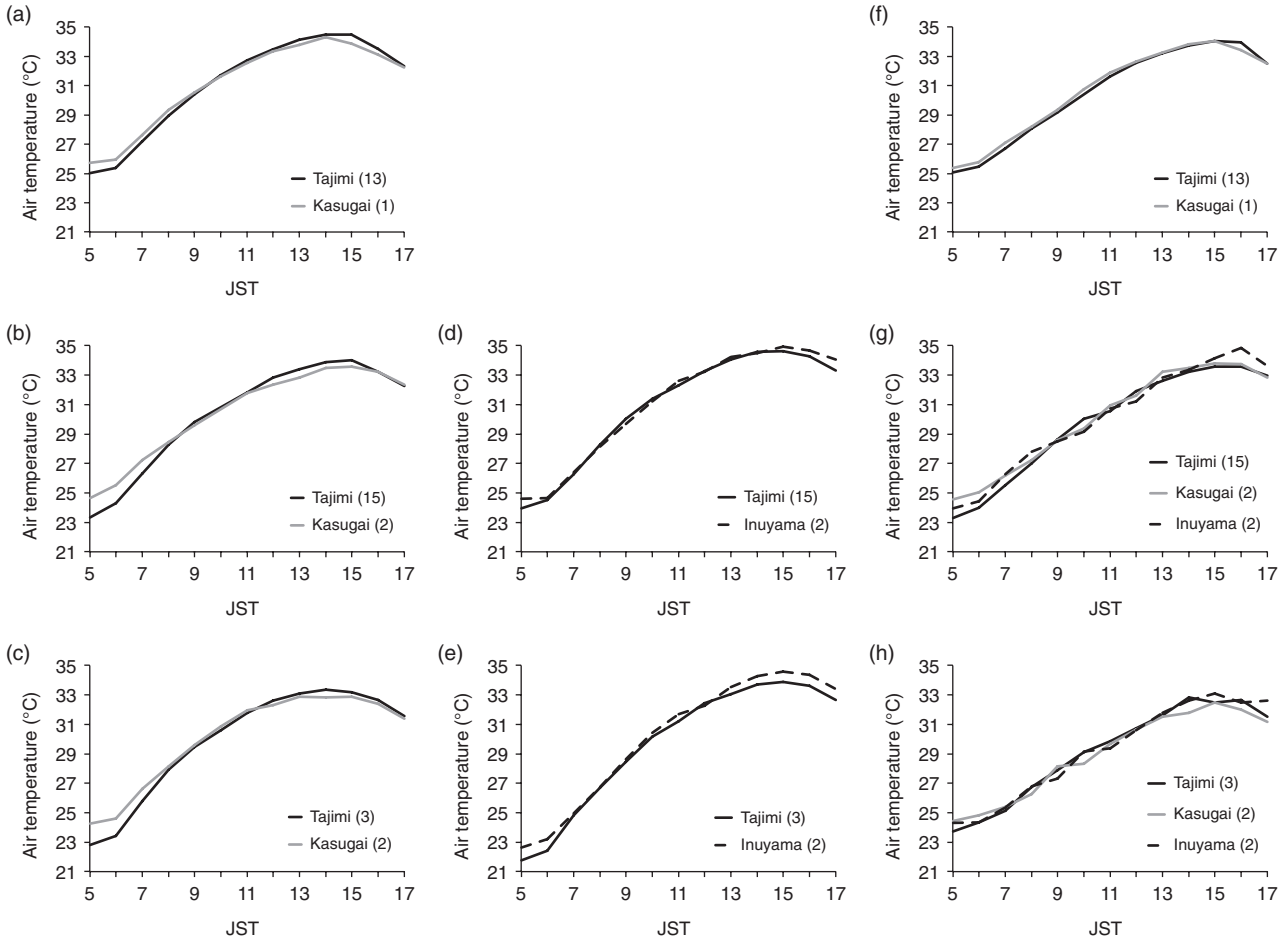

Figure 10. Averaged diurnal variation in surface air temperature from 0500 to 1700 JST for (a)–(c) southwesterly wind days, (d) and (e) westerly wind days, and (f)–(h) weak-wind days in August 2010 (above), July–August 2011 (middle), and July–August 2012 (bottom) in Tajimi (black solid lines), Kasugai (grey solid lines), and Inuyama sites (black dashed lines). The numbers in brackets represent the average at the sites.

for 2010 because no observation was made in August 2010 in Inuyama. These figures indicate that there was almost no difference in temperature between Inuyama and Tajimi (Figure 10(d)) in July–August 2011. In contrast, in July–August 2012, the temperature was slightly higher in Inuyama compared to Tajimi (Figure 10(e)). Based on these results, it is impossible to say that we detect foehn effects induced by the mountains surrounding Tajimi.

In this study, we defined a 'weak-wind day' as a day when the wind speed at 1400 JST in Tajimi was lower than the average wind speed within the 'clear-sky days' category. Figure 10(f) shows the time variation of temperature averaged over the weak-wind days in August 2010 in Kasugai and Tajimi. This figure demonstrates that there is almost no difference in the daytime temperatures between the two cities. Similarly, no remarkable temperature difference was found for weak-wind days in July–August 2011 (Figure 10(g)) and in July–August 2012 (Figure 10(h)). Based on these results, it is clear that the effect of rising temperatures due to thermally induced local circulation on weak-wind days in hypothesis (4) does not play a significant climatological role in the EHT events in Tajimi. This result is consistent with the results from model studies, based on a two-dimensional idealized basin, conducted by Kimura and Kuwagata (1995) – the amount of sensible heat accumulated in the column atmosphere in the valley is proportional to the height of the mountain surrounding the basin when the valley width is constant. In other words, since the average height of the mountains around Tajimi basin is low (200 m), the amount of sensible heat accumulated in the column atmosphere of the basin may be smaller than in the case of a basin with a higher elevation, which is why temperatures in the basin do not rise as significantly as those outside the basin.

Next, we investigated the formation of stagnant air areas in the Tajimi basin. In general, stagnant air near the ground surface contributes to the trapping of heat within the basin due to the inhibition of heat exchange between the bottom and the region above the basin. Therefore, we used the surface wind speed (number of weak-wind days) as an index of stagnant air near the ground surface. Figure 11 shows the probability of the occurrence of weak-wind days at each AMeDAS site for all days, clear-sky days, and EHT days. Weak-wind day were defined, in the same way each day at each site in the area shown in Figure 11 as slower than the average wind velocity at 1400 JST recorded at each site for all days, clear-sky days, and EHT days. The vectors in the figures denote the average

wind velocity at 1400 JST for each category, similar to Figure 8. Figure 11(a)–(c) reveals that the probability of a weak-wind day occurring in Tajimi declines from all days, to clear-sky days, to EHT days. This result indicates that weak winds occur less frequently than usual on EHT days in Tajimi. In addition, the average wind speed at 1400 JST in Tajimi on EHT days was higher than that across all days and on clear-sky days. These results demonstrate that the air near the ground in Tajimi is not climatologically stagnant on EHT days. However, it should be noted that these analyses merely show the climatological features of winds at the altitude of the anemometer placed at each AMeDAS site (e.g. 10 m at the Tajimi AMeDAS site). In general, the altitudes of the anemometer and thermometer were different. Therefore, detailed investigations should be carried out at an altitude below that of the anemometer. For instance, the climatological features of winds at ~1.5 m, where the thermometer is placed, should be elucidated.

We next consider hypothesis (5): the effect of UHI in Tajimi. Figure 12 shows the results of observations conducted within Tajimi in August 2010 and July–August 2011. Since the results of observations in July–August 2012 were obtained from only three observation sites (Table 2), these results are not shown. The results of observations in August 2010 reveal that UHI were located at Tajimi JR (Japan Railway) Station (site 10) and at Seika JS (site 7), at 0500 JST [Figure 12(a), similar to that indicated by Okada *et al.* (2014)]. High temperatures extended from 1400 JST from the downtown area, where Tajimi JR Station is located, to the entire area of the basin (Figure 12(b)). Similar characteristics were also observed in July–August 2011 (Figure 12(c) and (d)). As a special note on the observations conducted in 2011, the highest temperature was recorded near the AMeDAS site (site 14) at 1400 JST, which will be discussed more extensively in Section 3.4.

Yoshida (2013) mentioned that a reduction in the total area of rice paddy fields in the city during recent years is one of the factors implicated in the frequent occurrence of EHT events in Tajimi. Moreover, he pointed out the possibility that a decrease in precipitation and soil moisture contribute to EHT events. Here, we examine hypothesis (6): the effects of atmospheric conditions on soil dryness. Figure 13(a)–(c) shows the anomalies of the number of clear-sky days, 'cloudy days', and 'rainy weather days' at each observation site compared to the area-averaged number of such days at all the sites indicated in the figures. Cold (warm) colour sites denote fewer (more) clear-sky, cloudy or rainy weather days were observed than the area-averaged number. A 'rainy weather days' was defined as a day on which total precipitation was over 0.1 mm, and a 'cloudy day' was one that could not be classified as either a clear-sky day or a rainy weather day. Figure 13(a) indicates that the number of clear-sky days in Tajimi was greater than the area average. However, the anomaly is only +1 day. Additionally, the number of cloudy days in Tajimi was ~1 day less than the area average (Figure 13(b)). The number of rainy weather days in Tajimi was ~1 day more than the area average

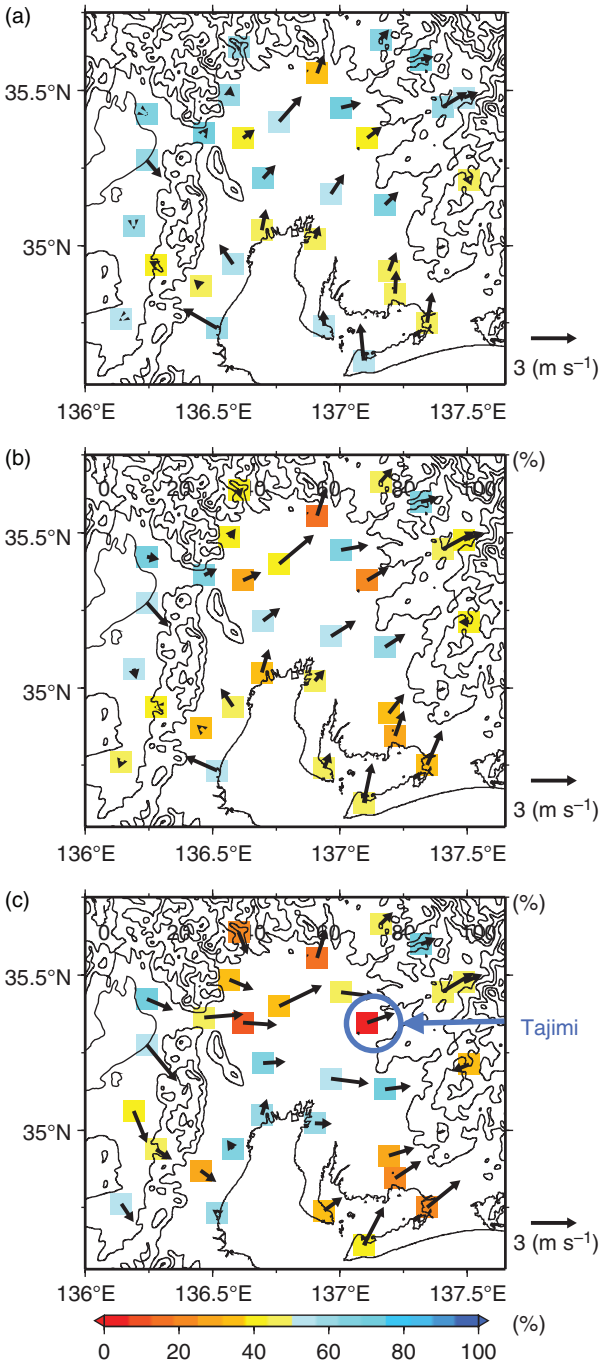

Figure 11. Horizontal distributions of probability of occurrence of weak wind days (colour), and averaged wind speed and direction (vector) at 1400 JST on (a) all days, (b) clear-sky days, and (c) EHT days.

(Figure 13(c)). These anomalies are very small and from the standpoint of atmospheric conditions, these results reveal that Tajimi is not in a condition that tends to result more in soil dryness than are its adjacent sites.

As one of the factors involved in the occurrence of EHT events, Fujibe (1996), Takane and Kusaka (2011), and Takane *et al.* (2014) also mentioned soil dryness caused by the consecutive clear-sky days preceding EHT events. With this in mind, Figure 13(d) shows the average number of consecutive clear-sky days prior to the occurrence of each EHT in Tajimi. As described in the previous figures,

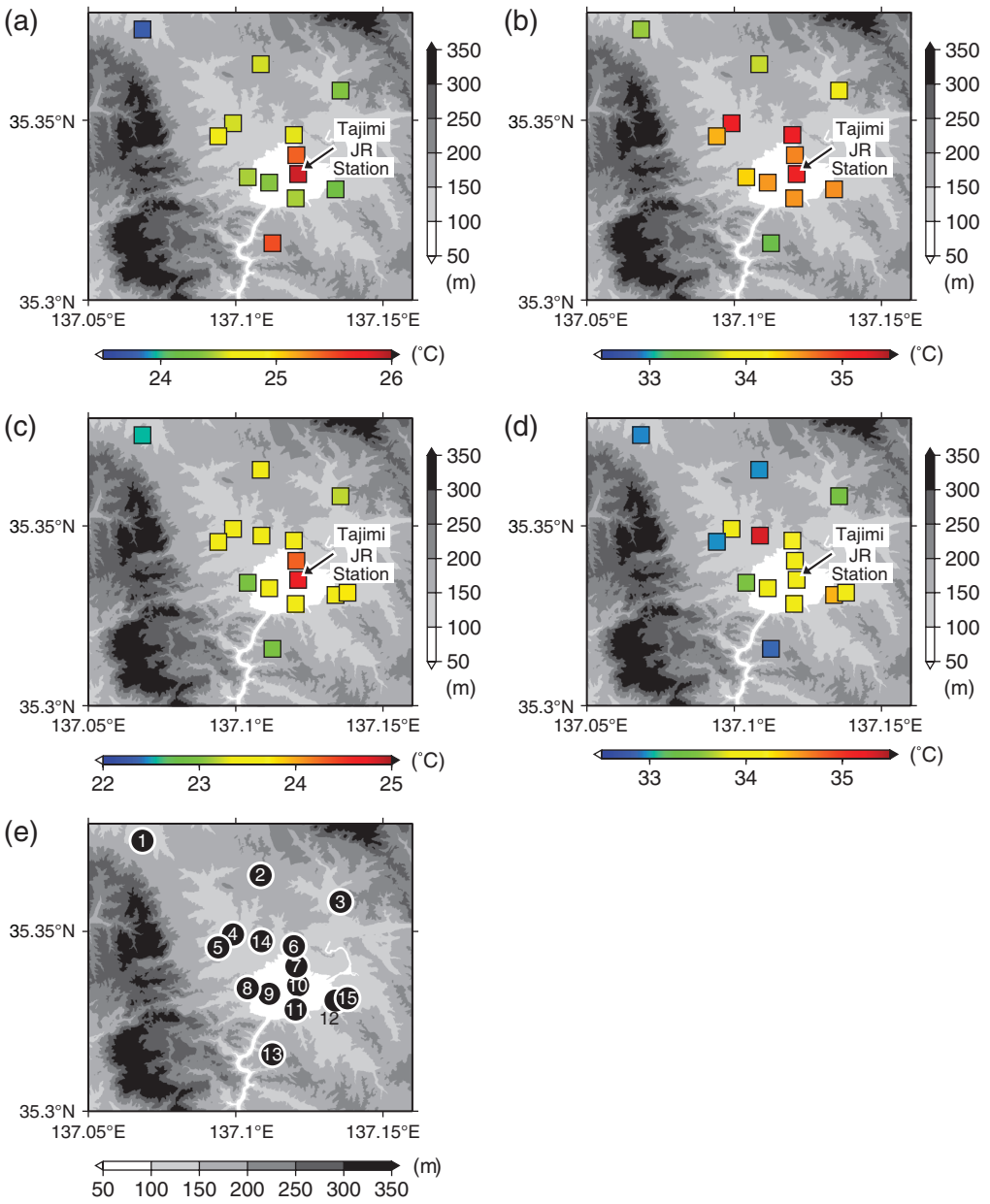

Figure 12. The spatial distribution of surface air temperature (colour) in Tajimi City at (a) and (c) 0500 and (b) and (d) 1400 JST averaged for clear-sky days in August 2010 (top), and July–August 2011 (bottom). (e) The locations of observation sites in Tajimi City are shown in Table 2, which is the same as Figure 2(c).

a lower (greater) number of consecutive clear-sky days was observed at each site indicated with cold colours (or warm colours) than the area-averaged number of clear-sky days. This figure indicates that the number of consecutive clear-sky days in Tajimi is about 2 days lower than the area average. This result means that a lower number of clear-sky days precede EHT events than the area average in Tajimi, suggesting that soil dryness associated with consecutive clear-sky days does not play a role in the occurrence of EHT events in Tajimi.

3.4. Micro-scale

The last section of this chapter discusses hypothesis (7): thermal environments around the Tajimi AMeDAS site (Figure 3(d)). Not only researchers but also citizens of Tajimi City have pointed out that undesirable micro-scale conditions at the Tajimi AMeDAS site are one reason for the higher temperatures recorded in Tajimi. Fujibe (2011) explained the 'Hidamari (suntrap) effect' mentioned in Section 1 as follows: 'Kondo has presented observational evidence of temperature changes that are apparently related to changes in the micro-scale environment (such as the construction of buildings, tree growth, reclamation and earthquake disasters). Kondo has noted that a decrease in exposure to the wind is accompanied by a reduction of wind speed and upward heat diffusion, which results in a temperature increase'. In general, AMeDAS observation sites were built nationwide by the JMA, and observation sites managed by JMA local observatories are generally constructed in open spaces with a relatively high

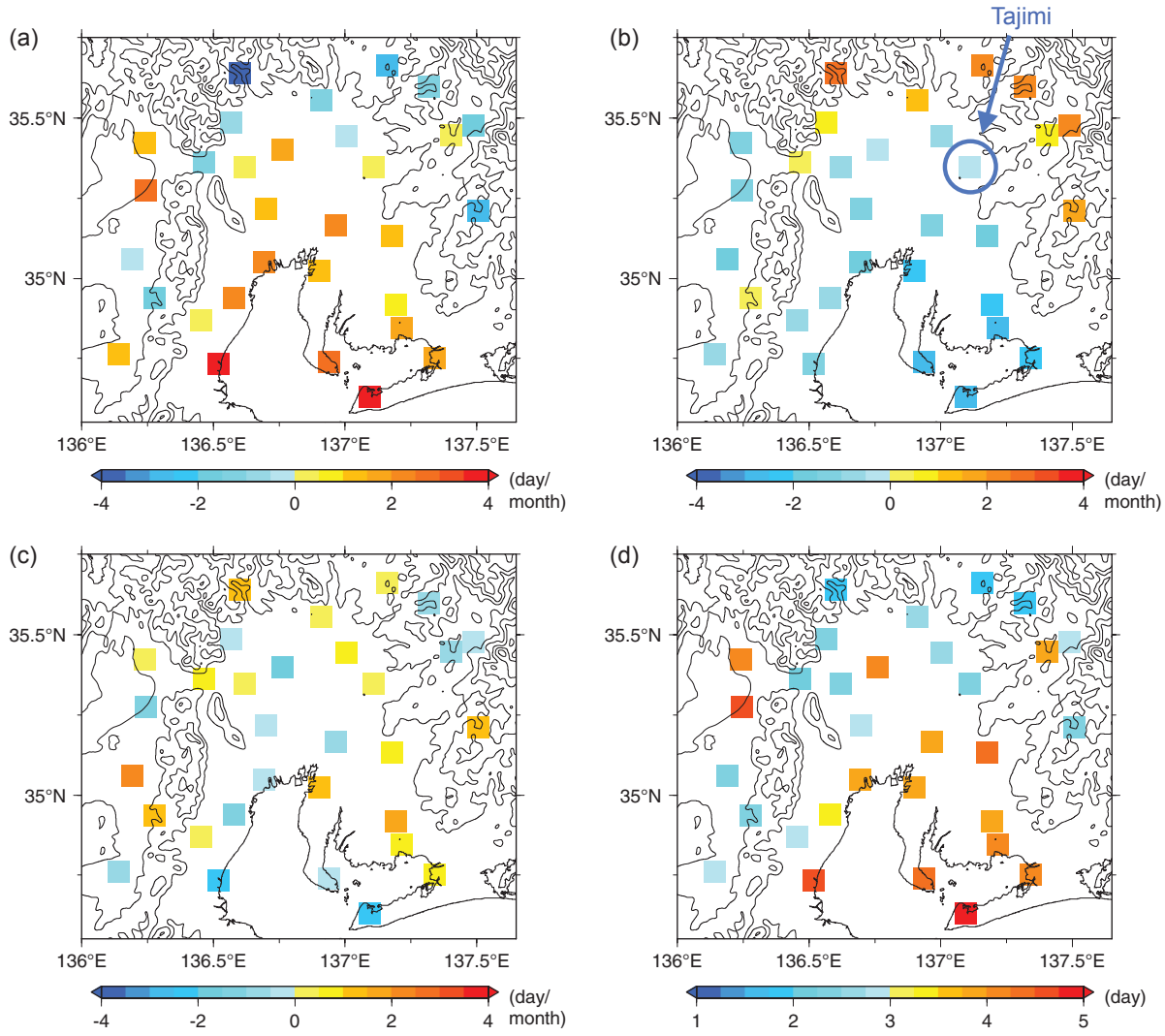

Figure 13. Horizontal distribution of anomalies in (a) clear-sky days, (b) cloudy days, and (c) rainy weather days. (d) Distribution of averaged preceding consecutive clear-sky days before EHT days in Tajimi.

sky view factor [e.g. Kumagaya site: Figure 2 in Takane *et al.* (2014)]. However, since the Tajimi AMeDAS site is not located in an open space (Figure 14), the question remains whether or not the temperatures observed at the site are representative of the thermal environments in Tajimi City. This is a possible explanation for high temperatures being more frequently observed at the Tajimi AMeDAS site. In recent years, the transition in thermal environments at the micro-scale level has been considered one of the important factors for global warming monitoring (Mahmood *et al.*, 2006; Runnalls and Oke, 2006; Pielke *et al.*, 2007; Fujibe, 2011). Thermal environments around meteorological observation sites have an impact not only on global warming monitoring but also on the frequency of EHT occurrences.

Thus, this article first investigates the differences in the locations of the temperature observations and their surrounding environments, and how these differences are related to the dispersion of the temperatures observed in the city (the uncertainty of temperatures recorded in Tajimi City). Figure 15(a) and (b) shows the averaged diurnal variations in temperature for clear-sky days recorded in Tajimi City at 13 sites and Tajimi AMeDAS site (as a reference) in August 2010, and 15 sites and Tajimi AMeDAS site in July–August 2011, all between 0500 and 1700 JST. In August 2010, 35.3 °C was the highest temperature recorded in Tajimi at 1400 JST (recorded in Koizumi Park: site 4), and the lowest temperature at the same hour was 33.8 °C (observed at Wakinoshima JS: site 13). The difference between the highest and the lowest temperature at 1400 JST was 1.5 °C, which is the range of uncertainty for temperature observation in the city. If altitude corrections were not applied, the difference would be 2.0 °C. In July–August 2011, the highest temperature in Tajimi City at 1400 JST was 35.3 °C (recorded near the AMeDAS site: site 14), and the lowest temperature was 33.1 °C (observed at Koizumi JS: site 5). The difference between the highest and lowest temperatures at 1400 JST was 2.2 °C, and was even greater (2.4 °C) when the altitude correction was not applied. Here again, the results of observations in July–August 2011 indicate that temperatures observed near the AMeDAS site were higher

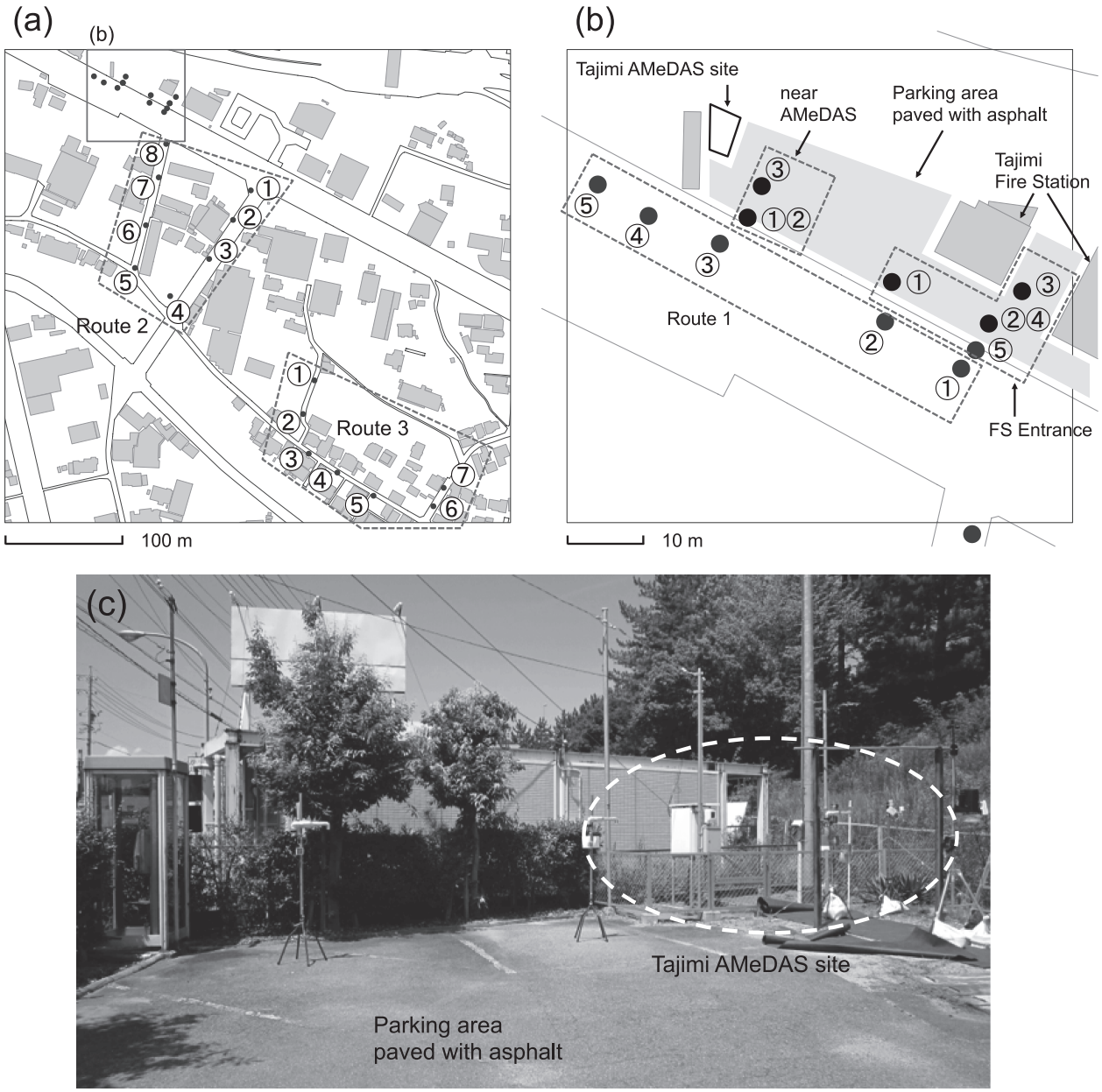

Figure 14. (a) Map of urban area in the vicinity of the Tajimi AMeDAS site. (b) Close-up of black square area identified in (a). (c) Photograph of Tajimi AMeDAS site taken from parking area of Tajimi fire station. The numbers from 1 to 8 in (a) and (b) represent the observation points on several routes: near AMeDAS, at the FS entrance, and routes 1–3.

than those observed at any other site in the city. In other words, near the AMeDAS site, temperatures tended to be higher than at other sites in the city, therefore this site is less regionally (Tajimi City) representative.

Second, we conducted intensive observations of temperature near AMeDAS and on peripheral city blocks, using a forced ventilation device (Murakami and Kimura, 2010), to investigate whether the temperature observed at the AMeDAS site was regionally representative a several-metre scale or several-hundred-metre city-block scale. For intensive observations, we conducted mobile observations on each of the following five routes: near AMeDAS (three sites: Figure 14(b)); at the fire station (FS) entrance (five sites: Figure 14(b)); on route 1 (five sites, Figure 14(b)); on route 2 (eight sites: Figure 14(a)); and on route 3 (seven sites, Figure 14(a)). Here, we explain the mobile observation method used in detail along route 2. We first stayed for 15 s on every hour at point ① on the route, and then conducted observations per second using the forced ventilation thermometer. These 15 data were then averaged, and were designated as the value for that particular point on the route. Subsequently, we took 30 s to move to point ②, where we conducted the same observation by standing still for 15 s. This process was repeated until we reached point ⑧. Points ①–⑧ were named the 'outbound' route. We then conducted the same observations from points ⑧ to ①, and labelled this the 'inbound' route. A total of 11 min of observations were

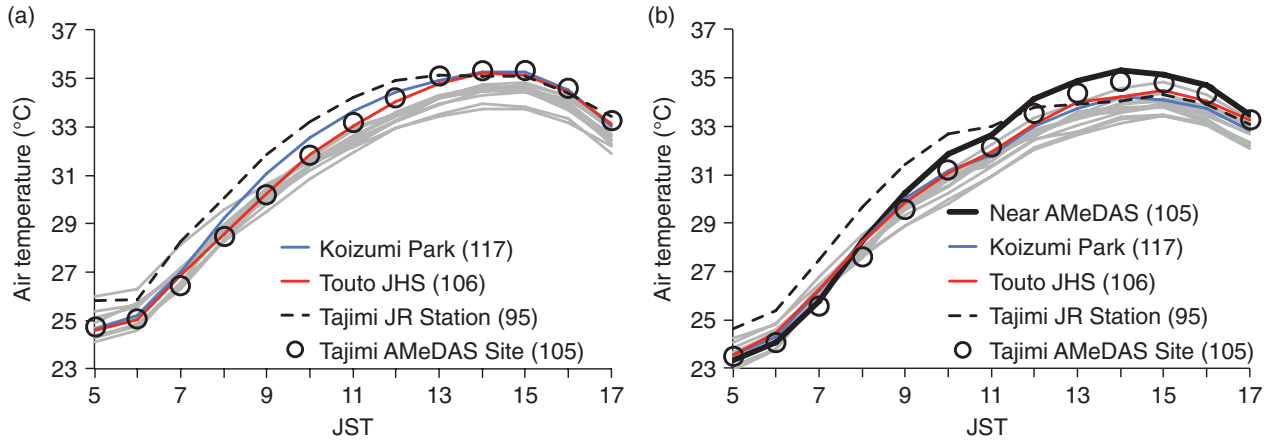

Figure 15. Averaged diurnal variation in surface air temperatures from 0500 to 1700 JST for clear-sky days in (a) August 2010 and (b) July–August 2011 at: near AMeDAS (black solid line); Koizumi Park (blue solid line); Touto JHS (red solid line); Tajimi JR station (black dashed line); Tajimi AMeDAS site (circle, as a reference); and other points (grey solid lines).

conducted on both the inbound and outbound routes along route 2, which had the maximum number of observation points among all routes. Such observations were then conducted on the other routes, using the same time interval on 12–14 August 2011: these 3 days were not considered EHT days, but were clear-sky days.

The results of the 15 s inbound and outbound average values obtained at the points on each route [for route 2, the result is of averaging the values for 16 points: 8 points × 2 (inbound and outbound)] are shown in Figure 16. The bars indicate the average surface air temperatures, while the error bars show their standard deviations. Figure 16(a) describes the results on 12 August 2011. While it appears that the average temperatures near AMeDAS at 1100 JST are at most about 0.5 °C higher compared to the values obtained for the other routes, the figure does not show this trend in observations conducted after 1200 JST, where the average temperatures near AMeDAS were considerably higher than those recorded on other routes. In addition, the standard deviations for the average temperatures near AMeDAS were neither lower nor higher than those for the other routes. Similar trends were also confirmed in the results for the observations conducted on 13 August 2011 (Figure 16(b)) and on 14 August 2011 (Figure 16(c)). In other word, daytime temperatures observed at near AMeDAS were not higher compared to the values obtained for the other routes during the 3 days.

Additional observation show that the average temperatures observed near AMeDAS between 1100 and 1600 JST by 'fixed point' observation (different observation from intensive observations presented earlier) using the forced ventilation thermometer, were confirmed to be 1.2–1.3 °C higher than those observed in Koizumi Park (site 4; fixed point observation) during the same hours for the 3 days. These results indicate the possibility that the thermal environment around the AMeDAS point may be less regionally representative at a several-hundred-metre city-block scale, including all routes shown in Figure 14, than on a several-metre scale (distance between near AMeDAS and Koizumi Park).

4. Discussion

4.1. Climatological comparison of the Nobi and Kanto Plains

Section 3.1 discussed how the probability of the 'whale' pressure pattern occurring is higher on EHT days than that on clear-sky days. In addition, it was explained that one of the characteristics of 'whale' is higher temperatures at the 850-hPa level, and that synoptic-scale winds above central Japan tend to be covered by westerly to northwesterly winds. These features are similar to those in the Kanto Plain (Takane *et al.*, 2014), and the reason for this similarity is that the distance between the two plains is small in synoptic-scale terms; the distance between Nagoya in the Nobi Plain and Tokyo in the Kanto Plain is ∼260 km. In addition, these two plains have similar geographical characteristics: i.e. mountain ranges are located to the northwest of both plains, which is the windward direction under the 'whale' pressure pattern. These results demonstrate the possibility that EHT events occur on the leeward side of mountains located in the west and northwest of the plains in central Japan, due to airflow over the mountains.

However, the probabilities of westerly–northwesterly meso-β-scale airflow on EHT days differ between Tajimi in the Nobi Plain and Kumagaya in the Kanto Plain, although synoptic-scale pressure patterns are similar in both plains. Specifically, the probability of westerly–northwesterly airflow in Tajimi was 61.2%, as shown in Section 3.2, which is higher than the 10.7% in Kumagaya reported by Takane *et al.* (2014). A potential reason for this probability difference is the difference in the height of the mountains located in the west and northwest side (windward direction under the 'whale') of both plains: the Ibuki mountainous area (Figure 1(b)) is lower than the Chubu mountainous area. When synoptic-scale wind speed and atmospheric stability are almost identical in both windward areas, airflow over the mountains in the Nobi Plain occurs more frequently than in the Kanto Plain. The probability difference in the westerly–northwesterly meso-β-scale airflow (over the mountains) affects the

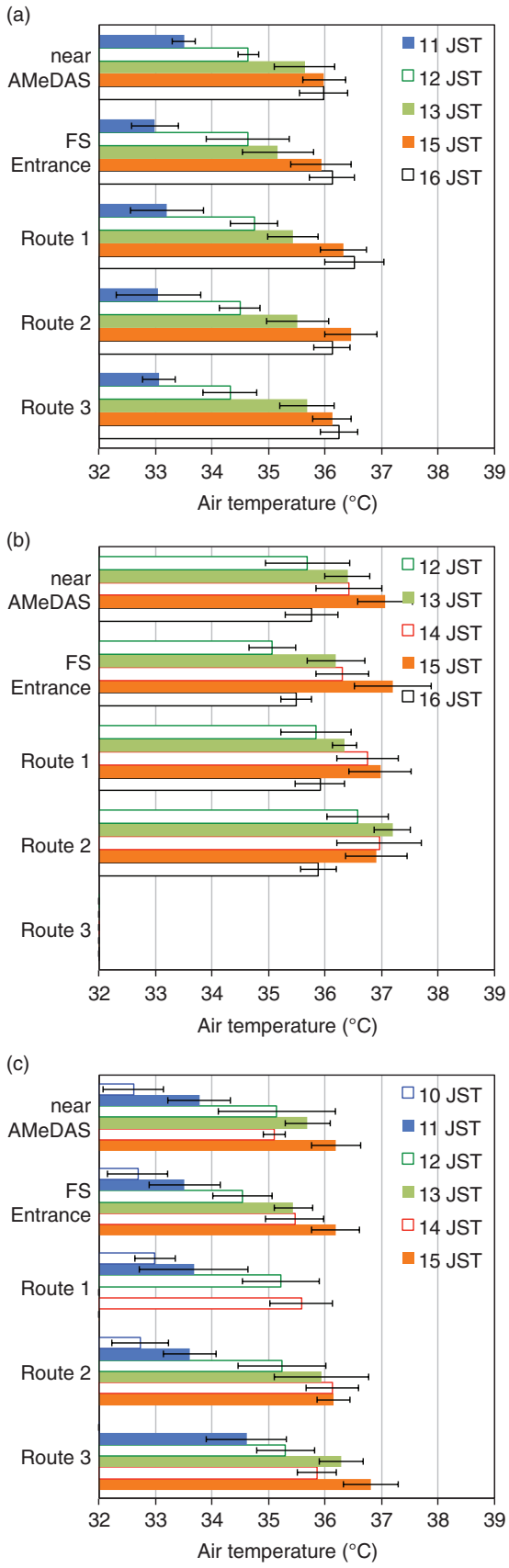

Figure 16. Averaged surface air temperatures (bars) and standard deviations (error bars) observed from 1000 to 1600 JST at: near AMeDAS; the FS entrance; and routes 1–3 (Figure 14), on (a) 12, (b) 13, and (c) 14 August 2011.

difference in the EHT frequency between Tajimi and Kumagaya (Table 1).

4.2. Identification of the meso-β-scale westerly–northwesterly wind

In this section, we discuss the difference in meso-β-scale airflow (coming from the mountains) between the northwestern and western sides of the Nobi Plain. Figure 9(c) shows that the temperature difference between Sekigahara and Ogaki (Figure 1) was 1.6 °C; Ogaki is located to the east of Sekigahara. The accumulated sunshine duration from sunrise to 1400 JST at Sekigahara and Ogaki showed no difference, 7.5 h. This suggests that the temperature difference between Sekigahara and Ogaki may be attributed to the foehns associated with the airflow passing through a col near Sekigahara. This westerly airflow entering the Nobi Plain eventually reaches Tajimi located at the east edge of the Nobi Plain. During this process in the Nobi Plain, the westerly winds are exposed to diabatic heating upon flowing in the mixed layer, causing high temperatures particularly at the end of the leeward side. The fetch to the westerly winds to Tajimi is greater than that for other cities (Sekigahara, Ogaki, and Gifu) in the Nobi Plain, and therefore, the duration of diabatic heating from the ground surface is longer for Tajimi than for other cities on the Nobi Plain. This mechanism corresponds to the foehn-like wind reported by Takane and Kusaka (2011). This could contribute to EHT events in Tajimi. Further detailed research should be conducted to analyse soil moisture, sensible heat flux, and other meteorological elements in the fetch area, and to identify their relationship to EHT events in Tajimi, using both numerical simulations and observation.

Owada (1990) stated that the local winds, called the Ibuki–Oroshi and Suzuka–Oroshi, are prominent on the Nobi Plain, and that both are westerly local winds. However, the meso-β-scale airflow from the mountains located on the northwestern and western sides is believed to be a different airflow from these local winds, for the following reasons. According to Owada (1990), the Suzuka–Oroshi is a westerly wind. However, this wind is generated in the coastal area located in the southwestern part of the Nobi Plain, which differs from the inland part of the Nobi Plain indicated in this study. Moreover, the pressure pattern creating the environment for the occurrence of the Suzuka–Oroshi includes high pressure in the west and low pressure in the east (WH–EL), a cyclone on the Japan Sea (JC), a cyclone located off the south coast of Japan (SC), and cyclones on the Japan Sea and the south coast of Japan (JS-Cs) [Figure 4 in Takane *et al.* (2014)]. Such pressure patterns are different from that of the 'whale' pressure pattern, which sets up the environment for the airflow from the mountains on the northwestern and western sides, referred to in this study.

Ibuki–Oroshi is generated in an area similar to that discussed in Section 3.2. However, this wind becomes prominent primarily during the winter season, and related pressure patterns are similar to those of Suzuka–Oroshi.

Few studies have examined the relationship between the airflow coming from the mountains located on the

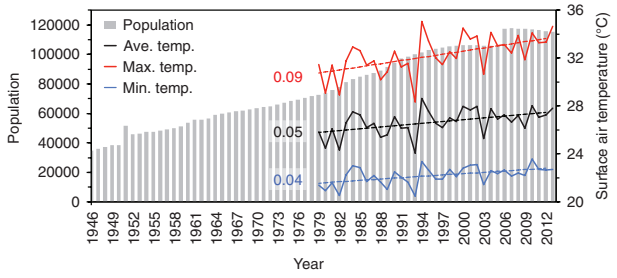

Figure 17. Secular change in population (grey bar) of Tajimi City from 1946 to 2012, daily average temperature (black solid line), maximum temperature (red solid line), and minimum temperature (blue solid line) observed at the Tajimi AMeDAS site, averaged for July–August in 1979–2012. The black, red, and blue straight, dashed lines indicate the trends in daily average, maximum, and minimum temperatures, respectively. The black, red, and blue numbers are the trends (°C year^{-1}).

northwestern and western sides, and the EHT days discussed in this study. This study indicates that the westerly–northwesterly wind is one of the factors causing the EHT events, and so further observational and numerical studies should be conducted to identify the physical characteristics of the westerly wind.

4.3. UHI in Tajimi City

As mentioned in Section 3.3, it appears that the UHI have contributed to changes in the occurrence of EHT events over the years. The population in Tajimi increased to approximately 80 000 people between 1946 and 2012 (Figure 17), and specifically by ∼38 000 between 1980 and 2012 (census data), which is a larger increase than in any other city in Gifu Prefecture in that time. Population growth has been evident in Koizumi school district (which houses sites 4 and 5) and Seika school district (which houses sites 14 and 7) since 1995. This localized urbanization within Tajimi City is believed to be one of the underlying factors for the occurrence of the EHT events around the Tajimi AMeDAS site in recent years.

In addition to the population increase in Tajimi, surface air temperatures (daily average, maximum, and minimum) averaged for July–August increased from 1979 (first year with observations available) to 2012 (Figure 17). The trends in daily average, maximum, and minimum temperature were +0.05, +0.09, and +0.04 °C year^{-1}, respectively. These positive trends included changes in temperature due to not only local phenomena, such as urban warming, but also global climate change. Here, we attempted to estimate the effects of local phenomena on the temperature trends listed earlier. This effect was estimated by subtracting temperature trends that were due only to global climate change (hereafter, background temperature change) from the temperature trends, which include both local phenomena and global climate change. Background temperature change was estimated using averaged observational data collected by 15 AMeDAS observational stations operated by the JMA, which were located outside urbanized areas in Japan. Additional analysis using the data from these stations revealed that the trends in the background temperature changes were +0.04 °C year^{-1} (daily average), +0.06 °C year^{-1} (maximum), and +0.03 °C year^{-1} (minimum). Therefore, the changes due to local phenomena only were +0.01 °C year^{-1} (daily average), +0.03 °C year^{-1} (maximum), and +0.01 °C year^{-1} (minimum). It can be seen that positive trends remain, despite the change in the background temperature. Considering that the population of Tajimi increased to approximately 43 000 people between 1979 and 2012 (Figure 17), and that the urbanized area of Tajimi expanded by about 3000 ha during the same period (city planning data from Gifu Prefecture), the positive trends due to local phenomena were affected by the urban warming of Tajimi. Specifically, changes in the ground surface energy budget due to land-use changes and an increase in anthropogenic heat due to urbanization contributed to the positive change in temperature and the increase in frequency of EHT events in Tajimi.

4.4. What are the important factors causing high temperatures in Tajimi?

The uniqueness of this study was its attempt to test seven climatological hypotheses, on different scales, which could explain the EHT events in the small city of Tajimi. The results of statistical analyses suggest that a combination of the following multi-scale factors contribute to the high temperatures in Tajimi. As shown in Section 4.3, urbanization of Tajimi City over several decades is a background factor in the high temperatures from a meso-γ-scale standpoint. In addition, the 'whale' pressure pattern is another background factor that triggers the higher temperatures. Under these background conditions, meso-β-scale westerly winds frequently blew at ground level in the Nobi Plain, and then reached Tajimi. This westerly–northwesterly wind is important for the EHT events in Tajimi. Moreover, the location of the Tajimi AMeDAS site, located within the urbanized area (a several-hundred-metre city-block scale) where high temperatures tend to be observed within the city, contributes to the high temperatures being recorded in Tajimi.

5. Summary

From the perspectives of various scales, this study investigated seven multi-scale-based hypotheses related to the occurrence of EHT events in one of the hottest cities in Japan, Tajimi City, in Gifu Prefecture, using results from original meteorological observations and from the JMA's observation data. The main results are summarized according to their hypotheses, as follows:

(1) A synoptic 'whale' pressure pattern had the highest probability of occurrence among all pressure patterns (a 61.2% probability of occurrence) on EHT days in Tajimi. This probability is significantly higher than the 11.3 and 21.0% on all days and clear-sky days, respectively. These results indicate that 'whale' plays a major role in the occurrence of EHT events, although it is neither a necessary nor a sufficient

condition to cause EHT events. In addition, the 'whale' pressure pattern is linked to the occurrence of the westerly–northwesterly meso-β-scale airflow.

(2) A 61.2% of EHT days had a prominent westerly–northwesterly airflow coming from the mountains located on the northwestern/western sides of the Nobi Plain. The observations suggest that the westerly–northwesterly airflow is closely related to EHT events and the 'whale' pressure pattern. Further research into the contribution of this westerly–northwesterly airflow is required, including the possible contribution of foehn-like winds, which cause high temperatures on the leeward side of the mountains, through diabatic heating from the ground surface.

(3) Prominent southwesterly winds from the Ise Bay area were observed on 12 of 49 EHT days (24.5%), showing that the probability of these winds was lower than that of the westerly winds on such days (61.2%). From a climatological perspective, these results suggest that it is less likely that hypothesis (3) – heat transport from Nagoya – contributes to the occurrence of EHT events in Tajimi.

(4) No tendency was found for temperatures in Tajimi (which is located inside a small-scale basin) to become higher than those observed outside the basin, due to small-scale foehn and valley winds induced by the mountains surrounding the city. In addition, formation of stagnant air areas was not observed. These results demonstrate that it is less likely that the small-scale basin terrain plays a role in the occurrence of EHT events in Tajimi.

(5) UHI was observed in Tajimi. As the population and surface air temperature of Tajimi has increased in recent decades, the urbanization of the city is a background factor, which is believed to have contributed to the increase in frequency of EHT events in the city.

(6) The number of clear-sky days in Tajimi was no greater than that of adjacent areas. Moreover, the numbers of cloudy days in the city was not less than in surrounding areas, and Tajimi had an only a slightly greater number of rainy weather days. These results indicate that Tajimi is not in atmospheric conditions where soil dryness tends to occur to a greater extent compared to its surrounding areas.

(7) The result of observations on clear-sky days in July–August 2011 suggest that higher daytime temperatures tend to be observed near the AMeDAS site compared to other sites within the city, and that this site is less regionally representative. The results of additional intensive observations indicate the possibility that the thermal environment around the AMeDAS site may be less regionally representative at the several-hundred-metre city-block scale than at the several-metre scale.

Based on these results, it is likely that the high temperatures in Tajimi can be attributed to: (1) the occurrence of a characteristic pressure pattern: 'whale', (5) the urbanization of the city as an underlying environment coupled with (2) the westerly–northwesterly airflow from the mountains located on the western/northwestern sides, and (7) the location of the AMeDAS site, which is located in a city block ($\sim$400 m^2) where high temperatures tend to be observed frequently within Tajimi City.

The statistical analysis presented here will be beneficial for understanding the climatological conditions during EHT events in other regions with similarly complex terrain, such as in south-eastern Asia and Europe.

Acknowledgements

This research was performed under a partnership agreement between the Center for Computational Sciences, University of Tsukuba and Tajimi City. We thank two anonymous reviewers for providing valuable comments that helped us to improve the manuscript. We thank Prof. Satoru Iizuka and members of Iizuka Laboratory of the Nagoya University, Mr Takayuki Kato of the University of Tsukuba, and Dr Yoshinori Shigeta of Risshou University (current affiliation: Tottori University of Environmental Studies), who helped to observation in several cities on the Nobi Plain during summer 2010–2012. We also thank Ms Reiko Kokubo of the University of Tsukuba for making several figures. This study was partially supported by the Research Program on Climate Change Adaptation of the Ministry of Education, Culture, Sports, and Technology, Japan, and JSPS KAKENHI Grant-in-Aid for Young Scientists (A) number 26702006. The data sets used for this study are provided from the cooperative research project of the JRA-25 long-term reanalysis by the JMA and the Central Research Institute of Electric Power Industry. The free software package Generic Mapping Tools was used in drawing the figures.

References

Beniston M. 2004. The 2003 heat wave in Europe: a shape of things to come? An analysis based on Swiss climatological data and model simulations. *Geophys. Res. Lett.* **31**: L102202, doi: 10.1029/2003GL018857.

Black E, Blackburn M, Harrison G, Hoskins B, Methven J. 2004. Factors contributing to the summer 2003 European heatwave. *Weather* **59**: 217–223.

Chase TN, Wolter K, Pielke RA Sr, Rasool I. 2006. Was the 2003 European summer heat wave unusual in global context? *Geophys. Res. Lett.* **33**: L23709, doi: 10.1029/2006GL027470.

Ciais P, Reichstein M, Viovy N, Granier A, Ogée J, Allard V, Aubinet M, Buchmann N, Bernhofer C, Carrara A, Chevallier F, De Noblet N, Friend AD, Friedlingstein P, Grünwald T, Heinesch B, Keronen P, Knohl A, Krinner G, Loustau D, Manca G, Matteucci G, Miglietta F, Ourcival JM, Papale D, Pilegaard K, Rambal S, Seufert G, Soussana JF, Sanz MJ, Schulze ED, Vesala T, Valentini R. 2005. Europe-wide reduction in primary productivity caused by the heat and drought in 2003. *Nature* **437**: 529–533, doi: 10.1038/nature03972.

De Bono A, Giuliani G, Kluser S, Peduzzi P. 2004. Impacts on summer 2003 heat wave in Europe. *UNEP/DEWA/GRID Eur. Environ. Alert Bull.* **2**: 1–4.

Fink AH, Brücher T, Krüger A, Leckebusch GC, Pinto JG, Ulbrich U. 2004. Factors contributing to the summer 2003 European heatwave. *Weather* **59**: 209–216.

Fujibe F. 1996. Boundary layer features of the 1994 hot summer in Japan. *J. Meteorol. Soc. Jpn.* **74**: 259–272.

Fujibe F. 2011. Urban warming in Japanese cities and its relation to climate change monitoring. *Int. J. Climatol.* **31**: 162–173, doi: 10.1002/joc.2142.

Grossman-Clarke S, Zehnder JA, Loridan T, Grimmond SB. 2010. Contribution of land use changes to near-surface air temperatures during recent summer extreme heat events in the Phoenix metropolitan area. *J. Appl. Meteorol. Climatol.* **49**: 1649–1664, doi: 10.1175/2010JAMC2362.1.

Hann J. 1866. Zur Frage über den Ursprung des Föhn. *Z. ÖBsterr. Ges. Meteorol.* **1**: 257–263.

IPCC. 2014. Summary for policymakers. In *Climate Change 2014: Impacts, Adaptation, and Vulnerability. Part A: Global and Sectoral Aspects. Contribution of Working Group II to the Fifth Assessment Report of the Intergovernmental Panel on Climate Change*, Field CB, Barros VR, Dokken DJ, Mach KJ, Mastrandrea MD, Bilir TE, Chatterjee M, Ebi KL, Estrada YO, Genova RC, Girma B, Kissel ES, Levy AN, MacCracken S, Mastrandrea PR, White LL (eds). Cambridge University Press: Cambridge, UK and New York, NY, 1–32.

Ito S, Iizuka S, Kuroki M. 2012. A sensitivity analysis of the factors in high temperatures in Tajimi by using WRF. *J. Environ. Eng. AIJ* **77**: 779–787 (in Japanese with English abstract).

Kimura F, Kuwagata T. 1995. Horizontal heat fluxes over complex terrain computed using a simple mixed-layer model and a numerical model. *J. Appl. Meteorol.* **34**: 549–558.

Kondo J, Kuwagata T, Haginoya S. 1989. Heat budget analysis of nocturnal cooling and daytime heating in a basin. *J. Atmos. Sci.* **46**: 2917–2933, doi: 10.1175/1520-0469(1989)046<2917:HBAONC>2.0.CO;2.

Kuwagata T, Kimura F. 1997. Daytime boundary layer evolution in a deep valley. Part II: Numerical simulation of the cross-valley circulation. *J. Appl. Meteorol.* **36**: 883–895, doi: 10.1175/1520-0450(1997)036<0883:DBLEIA>2.0.CO;2.

Li D, Bou-Zeid E. 2013. Synergistic interactions between urban heat islands and heat waves: the impact in cities is larger than the sum of its parts. *J. Appl. Meteorol. Climatol.* **52**: 2051–2064, doi: 10.1175/JAMC-D-13-02.1.

Mahmood R, Foster SA, Logan D. 2006. The GeoProfile metadata, exposure of instruments, and measurement bias in climatic record revisited. *Int. J. Climatol.* **26**: 1091–1124, doi: 10.1002/joc.1298.

Meteorological Society of Japan. 1998. *Encyclopedia of Meteorology and Atmospheric Sciences*. Tokyo Shoseki Co. Ltd.: Tokyo (in Japanese).

Murakami M, Kimura F. 2010. Manual of handmade field-portable forced ventilation thermometer. *Bull. Terr. Environ. Res. Cent. Univ. Tsukuba* **11**: 29–33.

Okada M, Kusaka H, Takaki M, Abe S, Takane Y, Fuji Y, Nagai T. 2014. Distribution of air temperature in Tajimi city in summer. *Tenki* **61**: 23–29 (in Japanese with English abstract).

Onogi K, Tsutsui J, Koide H, Sakamoto M, Kobayashi S, Hatsushika H, Mastsumoto T, Yamazaki N, Kamahori H, Takahashi K, Kadokura S, Wada K, Kato K, Oyama R, Ose T, Mannoji N, Taira R. 2007. The JRA-25 reanalysis. *J. Meteorol. Soc. Jpn.* **85**: 369–432, doi: 10.2151/jmsj.85.369.

Onuma K. 2003. Abnormal high temperatures cased by foehn wind in the Nohbi Plain. *J. Meteorol. Res.* **55**: 31–55 (in Japanese).

Owada M. 1990. *A Climatological Study of Local Winds (Oroshi) in Central Japan*. Doctoral Theses, Institute of Geoscience in University of Tsukuba, 98 pp.

Pielke RA, Davey CA, Niyogi D, Fall S, Steinweg-Woods J, Hubbard KK, Lin K, Cai M, Lim Y-K, Li H. 2007. Unresolved issues with the assessment of multidecadal global land surface temperature trends. *J. Geophys. Res.* **112**: D24S08, doi: 10.1029/2006JD008229.

Runnalls KE, Oke TR. 2006. A technique to detect microclimatic inhomogeneities in historical records of screen-level air temperature. *J. Clim.* **19**: 959–978, doi: 10.1175/JCLI3663.1.

Sakai S, Umetani K, Iizawa I, Ito A, Ono K, Yajima A, Amemura N, Morinaga S. 2009. Development of observational system for urban thermal environment. *Tenki* **56**: 337–351 (in Japanese with English abstract).

Schär C, Vidale PL, Lüthi D, Frei C, Häberli C, Liniger MA, Appenzeller C. 2004. The role of increasing temperature variability in European summer heatwaves. *Nature* **427**: 332–336, doi: 10.1038/nature02300.

Seibert RS. 1990. South foehn studies since the ALPEX experiment. *Meteorol. Atmos. Phys.* **43**: 91–103, doi: 10.1007/BF01028112.

Skamarock WC, Klemp JB, Dudhia J, Gill DO, Barker DM, Duda MG, Huang X-Y, Wang W, Powers JG. 2008. A description of the Advanced Research WRF version 3. NCAR Tech. Note NCAR/TN-4751STR, 113 pp. http://www.mmm.ucar.edu/wrf/users/docs/arw_v3.pdf (accessed 1 April 2015).

Takane Y, Kusaka H. 2011. Formation mechanisms of the extreme high surface air temperature of 40.9 °C observed in the Tokyo metropolitan area: considerations of dynamic foehn and foehnlike wind. *J. Appl. Meteorol. Climatol.* **50**: 1827–1841, doi: 10.1175/JAMC-D-10-05032.1.

Takane Y, Kusaka H, Kondo H. 2014. Climatological study on mesoscale extreme high temperature events in inland of the Tokyo metropolitan area, Japan, during the past 22 years. *Int. J. Climatol.* **34**: 3926–3938, doi: 10.1002/joc.3951.

Takane Y, Kusaka H, Kondo H. 2015. Investigation of a recent extreme high-temperature event in the Tokyo metropolitan area using numerical simulations: the potential role of a 'hybrid' foehn wind. *Q. J. R. Meteorol. Soc.* **141**: 1857–1869, doi: 10.1002/qj.2490.

Takane Y, Ohashi Y, Kusaka H, Shigeta Y, Kikegawa Y. 2013. Effects of synoptic-scale wind under the typical summer pressure pattern on the mesoscale high-temperature events in the Osaka and Kyoto urban areas by the WRF model. *J. Appl. Meteorol. Climatol.* **52**: 1764–1778, doi: 10.1175/JAMC-D-12-0116.1.

Yoshida N. 2013. Incentive award: features of abnormal high temperature events during summer in Tajimi city. *Tenki* **60**: 65–67 (in Japanese).